

THERMAL BEHAVIOR OF Cu(II)-, Cd(II)-, AND Hg(II)-EXCHANGED MONTMORILLONITE COMPLEXED WITH CYSTEINE

D. Malferrari¹, Maria Franca Brigatti^{1*}, Angela Laurora¹, L. Medici² and S. Pini¹

¹Dipartimento di Scienze della Terra, Università di Modena e Reggio Emilia, via S. Eufemia 19, 41100 Modena, Italy

²IMAA-CNR, Area della Ricerca di Potenza, Via S. Loja, 85050 Tito Scalo, Potenza, Italy

The thermal behavior of montmorillonite and organically modified montmorillonite, both treated with heavy metal cations [Cu(II), Cd(II) and Hg(II)], was characterized via thermal analyses (TG, DTG and DTA) combined with evolved species gas mass spectrometry (MS-EGA), and X-ray diffraction at in situ controlled temperature (HTXRD). The reactions involving Cu(II)- and Cd(II)-montmorillonite samples are mostly related to H₂O and OH loss, unlike Hg(II)-montmorillonite, where effects associated to Hg(II) loss are also present. Finally reactions related to dehydration, dehydroxylation and to organic matter decomposition can be observed in montmorillonite samples treated with cysteine.

Keywords: Cd(II), Cu(II), cysteine, Hg(II), mass spectrometry, montmorillonite, thermal analyses

Introduction

The layer in montmorillonite hosts several active structural sites. These latter can interact with ions in solution, thus imparting to the mineral both its well known sorptive properties toward inorganic cations and organic molecules, and the ability to control the diffusion and transport of heavy metals and organic contaminants [1]. Montmorillonite, or montmorillonite-like structures, are used as barriers to minimize contaminant transport from waste disposal sites [2]. The most effective active sites in montmorillonite are placed between two silicate layers (i.e., in the interlayer region), where the naturally occurring cations can easily be replaced by heavy metals and organic groups. Moreover, metals cations, especially transition metals in their upper oxidation state, can interact directly with organic solutes.

Other active sites can be originated from polarized water, surrounding exchangeable cations, and from hydroxyl groups located on the octahedral broken edges of the montmorillonite layer [3]. The binding of sorbed species on mineral surface usually depends on weak interactions such as van der Waals-London, hydrogen bonding, dipole-dipole and other electrostatic forces or entropy-driven hydrophobic bonding, thus not preventing an easy removal of the adsorbed species from the mineral surface even after limited variations in environmental conditions.

This background, also considering the wide application of montmorillonite and of montmorillonite-like minerals as barriers in waste disposal sites, clearly identifies the characterization of the adsorbed species and the description of the mineral layer structure thermal

evolution, as true key-points [4, 5]. This topic will be addressed in this work, where a detailed description of the thermal evolution of the montmorillonite layer, when hosting heavy metals and organic matter, will be provided. Heavy metals taken into consideration are Cu(II), Cd(II) and Hg(II). Copper is a common constituent of runoff from mining operations, of urban water runoff, and of industrial and agricultural effluents. Although in low concentrations Cu is essential to life, excessive Cu levels may be detrimental. Cu species can be differently adsorbed or bonded by montmorillonite in presence of water or organic molecules, also following complexation processes with organic matter [6]. Cadmium is a dangerous constituent of runoffs from industrial applications (see, for example nickel-cadmium batteries, pigments, metal coatings, alloys, and chemical stabilizers) [7]. Unlike many others transition metals that precipitate as hydroxides at pH values common in soils and surface waters, cadmium hydroxide is very soluble and its concentration in aqueous solutions does not appear to change appreciably up to pH=10 [8]. Furthermore different functional groups, such as metal complexing groups on montmorillonite surface, can enhance Cd(II) adsorption [9]. Mercury is one of the most serious contaminants in water and sediments. Even if present in traces, its high toxicity makes it a significant environmental threat [10].

Protein amino acids, which can naturally originate from the degradation of organic matter, play an important role in controlling environmental pollution, as demonstrated in various chemical, medical, biological and mineralogical investigations [5, 11]. Protein amino acids can bind metal cations via different func-

* Author for correspondence: brigatti@unimore.it

tional groups: via amino ($-NH_2$) and carboxylic ($-COOH$) groups, present in all species, and via sulfur-containing groups ($-SH$ and $-SCH_3$), which are specific for cysteine and methionine.

The thermal behavior of montmorillonite when Cu(II), Cd(II) and Hg(II) heavy metals and related metal-organic complexes are present will thus be described. Different experimental methodologies will be used, such as thermal analyses, mass spectrometry on evolved species during thermal reactions and X-ray diffraction at in situ controlled temperature.

Experimental

Materials

Montmorillonite sample

Montmorillonite STx-1 from Gonzales County Texas was provided by the Clay Minerals Society. The chemical composition is: $[IV]Si_{4.0}[VI](Al_{1.59}Fe^{3+}_{0.035}Fe^{2+}_{0.01}Mg^{2+}_{0.14}Ti_{0.01})[XIII](Ca_{0.12}Na_{0.035}K_{0.005})O_{10}(OH)_{22}$. Cation exchange capacity is 84.4 meq/100g. Further mineralogical and chemical details can be found in the report from the Clay Minerals Society [12]. Montmorillonite derives its layer charge mostly from low-charge cations sited in the octahedral sheet and can thus be considered as a soft Lewis base able to exchange soft acids, among which cations such as Cu, Cd and Hg [13].

Chemicals and solutions

All chemicals are analytical-grade reagents, not treated for further purification. Before starting experiments, the speciation of the heavy metals, involved in the reactions, was calculated via the MINTEQA2 program, to exclude the formation of precipitated phases on the montmorillonite surface [14].

Preparation of organically modified montmorillonite

A fixed amount of montmorillonite (50 g) was subjected to ultrasonic treatment, and the $<2\ \mu m$ size fraction was separated by sedimentation [15]. The clay sample was pretreated with 1 L of 1 M Na acetate solution [16]. The suspension was continuously shaken for 24 h at 50°C. After this time, the solution was removed and fresh Na solution was added. The procedure was repeated until X-ray results were consistent with Na-saturated interlayer (montmorillonite $d_{001}=13.1\ \text{\AA}$). After sedimentation and filtration of the suspensions, montmorillonite was air-dried and analyzed to check the completeness of Na exchange. Afterwards, a fixed amount of Na-exchanged montmorillonite (25 g) was dispersed in 0.5 L of 0.01 M cysteine solution. The starting pH value was adjusted

to 5.0, using acetic acid. During the experiment, pH was monitored continuously via a pH-meter (Jenway 3310) equipped with a glass electrode. The pH variation did not exceed ± 0.1 pH units.

Preparation of Cd, Cu, Hg saturated montmorillonite
Cd(II), Cu(II) and Hg(II) solutions (10^{-2} M) were used to obtain Cd(II)-, Cu(II)- and Hg(II)-treated montmorillonite and Cd(II)-, Cu(II)- and Hg(II)-organically modified montmorillonite. Sealed tubes containing 500 mg of montmorillonite (or organically modified montmorillonite) and 200 mL of each heavy metal solution were prepared. No constraints were imposed on pH during these isothermal reactions, but the starting and final pH values were recorded. Each system was shaken intermittently for a maximum period of 5 days. Three runs were made for each sample to determine the reproducibility and relative deviation of the experiments.

Methods

Elemental analysis (Elemental Analyzer, Carlo Erba 1106) was performed in order to check the amount of amino acid sorbed. An atomic absorption spectrophotometer (PerkinElmer Analyst 100) was used to analyze the amount of metal both in the mineral, after acid digestion, and in the solution. Standardized experimental procedures for each heavy metal were adopted.

X-ray powder diffraction at in situ high temperature (HTXRD) analysis was carried out in the temperature range $25 \leq T \leq 1100^\circ\text{C}$ on randomly oriented mineral aggregate mounts, using a Philips X'Pert PRO diffractometer equipped with X'Celerator detector (CuK α radiation; quartz as standard) and HTK16 Anton Paar heating apparatus.

Thermal analyses (DTA, TG and DTG) were performed with a Seiko SSC 5200 thermal analyzer equipped with a quadrupole mass spectrometer (ESS, GeneSys Quadstar 422) to analyze the gas phases evolved (MS-EGA) during thermal reactions. Gas phases were sampled via an inert, fused silicon capillary system, heated to prevent gas condensing. Gas analyses were carried out in Multiple Ion Detection mode (MID), which allows the qualitative determination of evolved masses vs. temperature or time. Background subtraction was performed to obtain the point zero condition before starting MID analysis.

Results and discussion

Montmorillonite structure can usually host heavy metal cations in two different locations: either at the interlayer position or at the octahedral broken edge faults [17, 18]. The first mechanism is more common than the second.

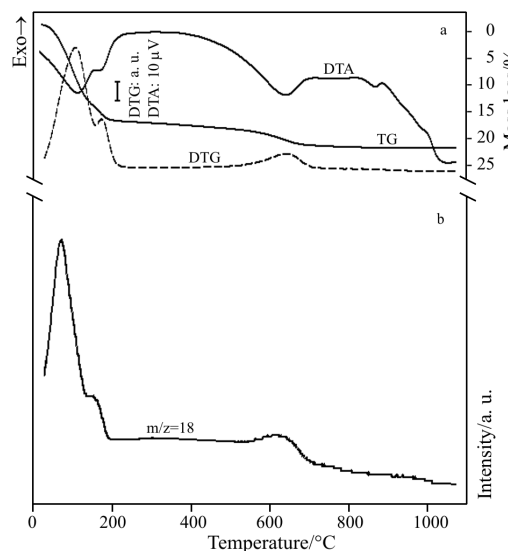


Fig. 1 a – TG, DTG, DTA curves and b – evolved gas masses of Cu(II)-montmorillonite

Thermal analyses for Cu(II)-montmorillonite sample (Fig. 1) show two endothermic reactions at about 114 and 179°C, related to weakly bonded water molecules as revealed from the analysis of the evolved gas ($m/z=18$, where m/z is the dimensionless ratio between the mass number and the charge number of an ion). The percentage of mass loss is 16.6 mass%. A further endothermic reaction, occurring in the temperature range $540 \leq T \leq 700$ °C, is due to the dehydroxylation of the octahedral sheet ($m/z=18$). The endo/exothermic reaction in the temperature range $830 \leq T \leq 900$ °C, not associated to mass loss, can be related to the formation of high temperature phases. At 1100°C the total mass loss is 21.9 mass%. Cd(II)-montmorillonite shows two endothermic reactions in the temperature range $25 \leq T \leq 200$ °C (Fig. 2). The first is at 75°C and the second at 155°C. Both effects are related to H_2O molecules loss ($m/z=18$; mass% = 12.2). A broad but unique dehydroxylation effect was registered at 670°C. The DTA curve shows at least two endo/exothermic effects in the temperature range $800 \leq T \leq 950$ °C. The different behavior of Cd(II)-montmorillonite, when compared to the natural sample, can evidence an interaction between Cd(II) and the silicate layer. At 1100°C the total mass loss is 16.8 mass%. For Hg(II)-montmorillonite (Fig. 3), the mass loss associated to dehydration is 8.1 mass% whereas an additional broad endothermic reaction (3.1 mass%) is associated to Hg loss ($m/z=199$). In the temperature range $400 \leq T \leq 1000$ °C, Hg(II)-montmorillonite shows a mass loss of 4.7 mass% following an endothermic reaction at 600°C related to the simultaneous evolution of H_2O ($m/z=18$) and Hg ($m/z=199$). A broad endothermic reaction is revealed at about 780°C (mass% = 0.8), due to Hg loss. A broad effect characterizes the DTA curve between 900 and 950°C. The total mass loss at 1100°C is 17.6 mass%.

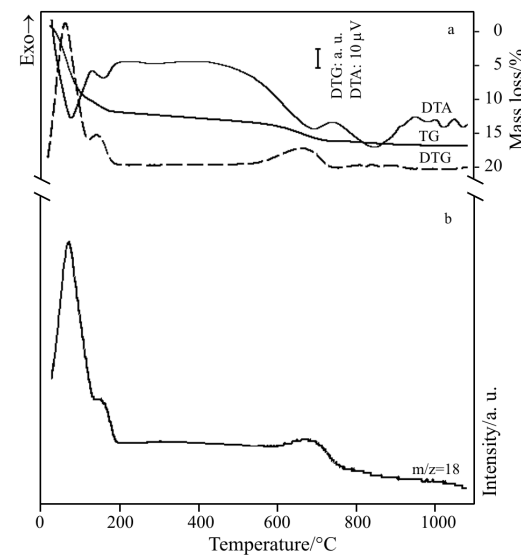


Fig. 2 a – TG, DTG, DTA curves and b – evolved gas masses of Cd(II)-montmorillonite

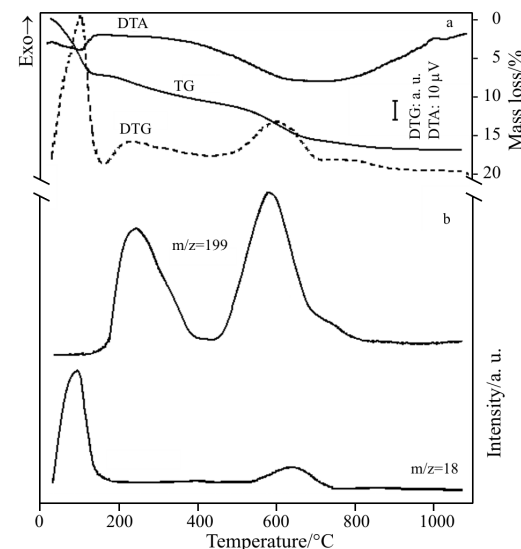


Fig. 3 a – TG, DTG, DTA curves and b – evolved gas masses of Hg(II)-montmorillonite

The thermal behavior of montmorillonite thus depends on the different treating heavy metal cation. A further insight can be gained, at temperature values below 250°C from EXAFS evidence. Cu(II) can be adsorbed by the montmorillonite layer as: *i*) dimmer or a combination of monomers and dimmers, linked by hydroxyl groups or by oxygen atoms at the mineral surface [19, 20]; *ii*) Cu(II)-water complexes, sited at the interlayer positions and showing a tetrahedral coordination with the first H_2O sheet. More H_2O sheets (1 or 2) can be coordinated with Cu(II) depending on environmental conditions. Cd(II) shows a tetrahedral coordination with four water molecules. A second layer of water molecules, less strongly bonded to the central cation, was also identified. Finally Hg(II) is

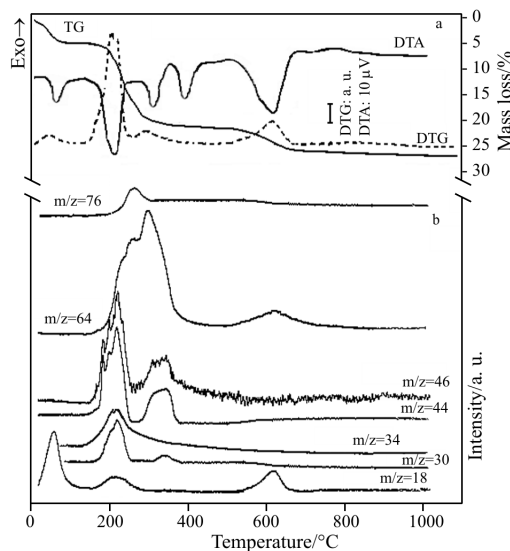


Fig. 4 a – TG, DTG, DTA curves and b – evolved gas masses of Cu(II)-cysteine-montmorillonite

present in montmorillonite structure in a deformed coordination, showing three shorter (1.99 Å) and three much longer distances (2.40 Å) [21].

The thermal behavior of Cu(II)-cysteine-montmorillonite complex, described by TG and MS-EGA analyses, shows that in the temperature range $25 \leq T \leq 150^\circ\text{C}$, the percentage of observed mass loss (8.9 mass%) corresponds to the release of H_2O molecules (Fig. 4). In the temperature range $150 \leq T \leq 400^\circ\text{C}$, the mass loss (17.2 mass%) is linked to the emission of H_2O ($m/z=18$), NO (or CH_3CH_3 , $m/z=30$), CO_2 ($m/z=44$), H_2S ($m/z=34$), NO_2 ($m/z=46$), SO_2 ($m/z=64$) and N_2O_3 ($m/z=76$). The DTA curve shows two endothermic reactions at 228 and 315°C both producing a mass loss, unlike a third endothermic reaction at 390°C. This reaction can probably be associated to the formation of residual, CuS like, interlayer phases derived from the decomposition of Cu(II)-cysteine complexes [20]. In the temperature range $525 \leq T \leq 650^\circ\text{C}$, the TG curve evidences a mass loss of 5.5 mass% which is usually attributed to the complete dehydroxylation of the smectite layer ($m/z=18$). The mass loss obtained for Cu(II)-cysteine-montmorillonite complex at 600°C, greater than in Cu(II)- H_2O -montmorillonite, can be related to the overlap of different dehydroxylation effects and to the emission of residual molecules present in Cu-cysteine complexes. The emission of SO_2 ($m/z=64$) at about 600°C may be attributed to the oxidation of these latter molecules [22].

The thermal behavior of the Cd(II)-cysteine-montmorillonite complex shows, in the temperature range $25 \leq T \leq 200^\circ\text{C}$, a decrease in mineral mass (9.5 mass%) related to the loss of H_2O molecules (Fig. 5). The mass loss is significantly less than in the sample treated with Cd(II) only (12.2 mass%). Furthermore the loss of H_2O molecules, like in the sample untreated with cysteine, is divided in two effects: the first

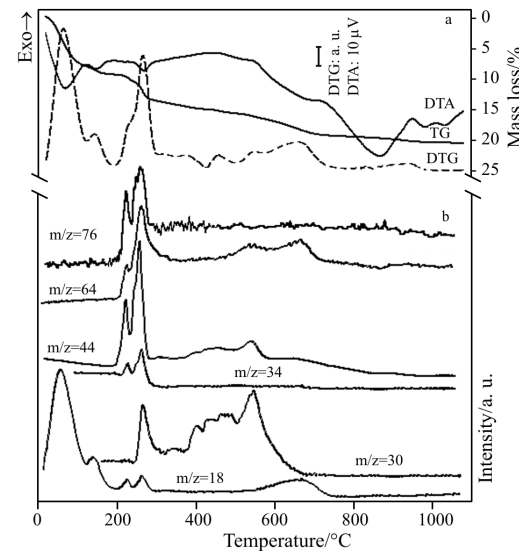


Fig. 5 a – TG, DTG, DTA curves and b – evolved gas masses of Cd(II)-cysteine-montmorillonite

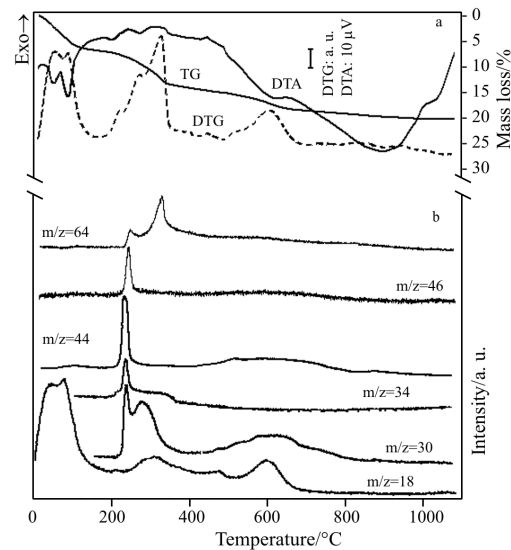


Fig. 6 a – TG, DTG, DTA curves and b – evolved gas masses of Hg(II)-cysteine-montmorillonite

at 75°C and the second at 155°C . In the temperature range $200 \leq T (\text{°C}) \leq 900$, the mass loss (10.6 mass%) is associated to different endothermic reactions which correspond to the release of: *i*) NO (or CH_3CH_3), H_2O , H_2S , CO_2 , SO_2 and N_2O_3 at 232 and 264°C ; *ii*) NO (or CH_3CH_3), CO_2 , and SO_2 at 549°C ; *iii*) H_2O and SO_2 at 673°C . The DTA curve shows broad endo-exothermic reactions in the temperature range $750 \leq T \leq 1100^\circ\text{C}$. At 1100°C the total mass loss is 20.6 mass%. The thermal behavior of Hg(II)-cysteine-montmorillonite complex (Fig. 6) evidences a mass loss of 7.4 mass%, before reaching 200°C , ascribed to dehydration. In the temperature range $200 \leq T \leq 900^\circ\text{C}$ different processes occur, accounting for a further mass loss of 12.7 mass%. In particular: *i*) two reactions, associated to amino-acid

decomposition, can be observed in the temperature range $250 \leq T \leq 350^\circ\text{C}$, as also revealed by the evolution of H_2O , NO (or CH_3CH_3), H_2S , CO_2 , NO_2 , and SO_2 phases; *ii*) a dehydroxylation reaction, concomitant to the decomposition of residual amino acid molecules (CO_2 and NO_2 or CH_3CH_3), can be observed at temperature values close to 600°C . It is worth noting that, unlike Cu(II)- and Cd(II)-cysteine-montmorillonite samples, the reaction associated to the evolution of SO_2 gas phases (temperature range $500 \leq T \leq 680^\circ\text{C}$) is missing, as well as the release of Hg, as observed in the montmorillonite sample treated with Hg only (temperature range: $200 \leq T \leq 800^\circ\text{C}$).

These results seem to suggest that Hg(II)-cysteine complexes, hosted in the montmorillonite interlayer, are characterized by extremely strong bonds, which are relatively stable at temperature values lower than the ones characterizing the formation of high temperature phases.

At room temperature and controlled relative humidity ($RH=60\%$), the (001) basal reflection for Cu(II)-, Cd(II)- and Hg(II)-montmorillonite is close to 15 \AA (Fig. 7). The transition to the dehydrated phase, which is revealed by the shift of (001) reflection to 10 \AA , occurs at about 220°C for Cu(II)- and Cd(II)-montmorillonite and at 180°C for Hg(II)-montmorillonite. A further reduction in layer thickness (9.6 \AA for Hg(II)-montmorillonite and 9.4 \AA for Cu(II)- and Cd(II)-montmorillonite, respectively) starts at about 400°C .

Dehydroxylation occurs at about 600°C , as revealed by the disappearance of (060) reflection. High temperature phases, such as cristobalite and corundum occur at about 700°C for Cu(II)- and Cd(II)-montmorillonite and 950°C for Hg(II)-montmorillonite. When metal-cysteine complex is present in the montmorillonite structure, the layer thermal history can be described as follows:

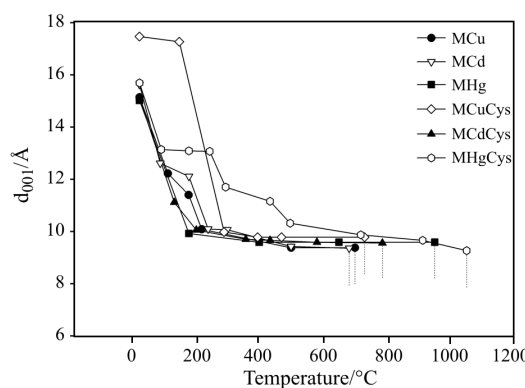


Fig. 7 d_{001} basal reflection (\AA) vs. temperature ($^\circ\text{C}$). Dashed lines indicate the formation of high temperatures phases. Labels: MCu=Cu(II)-montmorillonite; MCd=Cd(II)-montmorillonite; MHg=Hg(II)-montmorillonite; MCuCys=Cu(II)-cysteine-montmorillonite; MCdCys=Cd(II)-cysteine-montmorillonite; MHgCys=Hg(II)-cysteine-montmorillonite

- The Cu(II)-cysteine-montmorillonite complex is characterized by a d_{001} reflection value of 17.4 \AA at room temperature, which is reduced to 10 \AA at 280°C due to the emission of H_2O molecules (Figs 4 and 7). This d_{001} reflection value does not substantially change in position up to 700°C and disappears at 750°C , following the formation of high temperature phases (cristobalite and corundum).
- Cd(II)-cysteine-montmorillonite complex shows a basal periodicity of 15.1 \AA at room temperature. At 200°C , the emission of H_2O molecules produces a layer reduction ($d_{001}=10.2 \text{ \AA}$; Figs 5 and 7). A progressive reduction up to 9.8 \AA , associated to the emission of cysteine decomposition products, is then observed. The d_{001} reflection does not change from 9.8 \AA up to 750°C , even if its intensity progressively decreases. This reflection disappears at about 800°C , when reflections revealing corundum and cristobalite are identified.
- The Hg(II)-cysteine complex shows a basal periodicity of 15.6 \AA at room temperature. After temperature increase, a progressive reduction of basal periodicity takes place, namely: $d_{001}=13.2 \text{ \AA}$ from 100 to 245°C ; $d_{001}=11.7 \text{ \AA}$ at 300°C ; $d_{001}=11.2 \text{ \AA}$ at 435°C ; $d_{001}=10.3 \text{ \AA}$ at 500°C . No further variation in d_{001} value is then observed up to 720°C , where layer periodicity reduces to 9.6 \AA . At 1050°C , the d_{001} value is 9.34 \AA . At about 1100°C , the d_{001} reflection disappears, thus evidencing the formation of high temperature phases.

Conclusions

The thermal behavior of montmorillonite and organically modified montmorillonite, when exchanged with heavy metals, changes significantly as a function of the treating metal cation and of the presence of organic phases.

The sample treated with Cu(II) and cysteine is characterized at 600°C by the emission of H_2O , derived from dehydroxylation reactions, and of SO_2 . No emission of gas phases such as H_2S , N_xO_y and CO_2 is observed, thus evidencing a strong bonding between Cu and N (from the amino group) and between Cu and O (from the carboxylic group).

Previous works [18] suggested that Cu is not bonded to the thiol group at room temperature. Several hypotheses can thus be formulated to explain the emission of SO_2 at 600°C , namely: *i*) the formation of a strong bond between the dehydrated layer and S, which can thus be removed only at higher temperature; *ii*) the breaking of the bond between Cu and aminic and carbossilic groups, following the decomposition reaction at 200°C , thus leading to the formation of Cu_xS -like compounds. These latter are then subjected to decomposition reactions at higher temperatures with

the consequent emission of SO_2 and formation of mostly CuO as residual phase according to the reaction $2\text{CuS} + 3\text{O}_2 \rightarrow 2\text{CuO} + 2\text{SO}_2$. A similar reaction was previously observed [20, 22] in the range $330 \leq T \leq 420^\circ\text{C}$, when studying the decomposition of CuS in oxidizing environments. In this work sulfur emission was revealed at higher temperatures, probably due to the different environmental conditions, where the reaction progresses only when a sufficient amount of O_2 is rendered available by dehydroxylation reactions.

Sample treated with cysteine and Cd(II) shows the emission of NO (or CH_3CH_3), CO_2 and SO_2 in the range $400 \leq T \leq 600^\circ\text{C}$, thus evidencing the decomposition of the amino acid. This feature is evident for this sample only. Moreover results from X-ray analyses do not change appreciably in this temperature range (i.e., d_{001} position is almost constant). These reactions can thus be attributed to the decomposition of an organic fraction not strongly bonded to the mineral (e.g., adsorbed on the surface or present as a precipitated phase not revealed by diffraction). The emission of SO_2 and H_2O at temperature values slightly higher than 600°C can be explained following the same mechanism as described for montmorillonite treated with Cu(II) and cysteine.

Thermal analysis data for the sample treated with cysteine and Hg(II) do not reveal any significant difference with respect to the sample treated with Hg(II) only in the temperature range $25 \leq T \leq 400^\circ\text{C}$. However the thermal behavior is completely different at higher temperature values. A recent study [23], based on standard samples and soil from Hg contaminated areas, demonstrated that Hg is released after heating at different temperatures, depending on the binding functional groups. In HgS and HgO like phases, the metal vaporizes in the interval $200 \leq T \leq 300$ and $400 \leq T \leq 500^\circ\text{C}$, respectively.

Unlike the sample treated with Hg(II) only, the sample pretreated with cysteine never evidences the release of Hg ($m/z=199$). EXAFS studies identify S–Hg distances of 2.38 and 2.93 Å [21], thus suggesting that Hg complexation reactions involve both the thiol ($\text{R}-\text{SH}$) and the di-sulfuric and hydro-sulfuric groups ($\text{R}-\text{SS}-\text{R}$ and RSSH).

Acknowledgements

This work was made possible by the financial support of Ministero dell'Università e della Ricerca Scientifica of Italy, project 'Controllo dei fattori petrologici sulla cristallochimica delle miche'.

References

- 1 C. J. A. Appelo, Rev. Mineral., 34 (1996) 193.
- 2 R. W. Gullick, W. J. Weber and D. H. Gray, CMS workshop lectures, 8 (1996) 96.
- 3 D. L. Bish and G. D. Guthrie, Mineralogy of clay and zeolite dusts (exclusive of 1:1 layer silicates), Mineralogical Society of America, 1994, p. 139.
- 4 L. A. Pérez-Maqueda, V. Balek, J. Poyato, J. L. Pérez-Rodríguez, J. Šubrt, I. M. Bountseva, I. N. Beckman and Z. Málek, J. Therm. Anal. Cal., 71 (2003) 715.
- 5 Y. Xi, W. Martens, H. He and R. L. Frost, J. Therm. Anal. Cal., 81 (2005) 91.
- 6 K. Xia, W. Bleam and P. A. Helmke, Geochim. Cosmochim. Acta, 61 (1997) 2211.
- 7 A. L. Page, A. C. Chang and M. El-Amamy, in Lead, Mercury, Cadmium and Arsenic in the Environment, T. C. Hutchinson and K. M. Meema, John Wiley and Sons, New York 1987, p. 360.
- 8 B. C. Bostick, S. Fendorf and M. Fendorf, Geochim. Cosmochim. Acta, 64 (2000) 247.
- 9 I. Lagadic, M. K. Mitchell and B. D. Payne, Environ. Sci. Technol., 35 (2001) 984.
- 10 C. J. Watras and J. W. Huckabee, Mercury as a Global Pollutant: Towards Integration and Synthesis, Lewis Press, Boca Raton, FL 1994, p. 203.
- 11 V. Cody, X-ray crystal structure of amino acids and selected derivatives. In Chemistry and Biochemistry of Amino Acids, G. C. Barrett, Chapman and Hall, London, New York 1985, p. 684.
- 12 P. M. Costanzo and S. Guggenheim, Clays Clay Miner., 49 (2001) 371.
- 13 S. Xu and J. B. Harsh, Clay. Clay Miner., 40 (1992) 567.
- 14 J. D. Allison, D. S. Brown and K. J. Novo-Gradac, MINTEQA2/PRODEFA2, a geochemical assessment model for environmental system: version 3. 0, 1991, United States Environmental Protection Agency, Athens, Georgia 30613.
- 15 M. L. Jackson, in Soil chemical analysis, advanced course, 2nd Ed., M. L. Jackson, Madison Wisconsin, University of Wisconsin, 1975, p. 895.
- 16 J. Singh, P. M. Huang, U. T. Hammer and W. W Liaw, Clays Clay Miner., 44 (1996) 41.
- 17 A. Gupta, G. H. Loew and J. Lawless, Inorg. Chem., 22 (1983) 111.
- 18 T. Undabeytia, S. Nir, G. Rytwo, E. Morillo and C. Maqueda, Clays Clay Miner., 46 (1998) 423.
- 19 J. D. Morton, J. D. Semrau and K. F. Hayes, Geochim. Cosmochim. Acta, 65 (2001) 2709.
- 20 M. F. Brigatti, S. Colonna, D. Malferri and L. Medici, Geochim. Cosmochim. Acta, 68/4 (2004) 781.
- 21 M. F. Brigatti, S. Colonna, D. Malferri, L. Medici and L. Poppi, Appl. Clay Sci., 28 (2005) 1.
- 22 J. G. Dunn and C. Muzenda, Thermochim. Acta, 369 (2001) 117.
- 23 H. Biester, M. Gosar and S. Covelli, Environ. Sci. Technol., 34 (2000) 3330.

Received: September 25, 2005

Accepted: December 20, 2005

OnlineFirst: June 27, 2006

DOI: 10.1007/s10973-005-7327-y